



The treatment of bladder cancer in a mouse model by epigallocatechin-3-gallate-gold nanoparticles

Dar-Shih Hsieh^{a,b,1}, Hang Wang^{a,1}, Shan-Wen Tan^a, Yi-Huei Huang^a, Cheng-Yuh Tsai^a, Ming-Kung Yeh^c, Chang-Jer Wu^{a,*}

^a Department of Food Science, National Taiwan Ocean University, 2 Pei-Ning Road, Keelung, Taiwan

^b Division of Urology, Keelung Civilian Administration Division, Tri-Service General Hospital, National Defence Medical Center, Taipei, Taiwan

^c Institute of Preventive Medicine, National Defence Medical Center, Taipei, Taiwan

ARTICLE INFO

Article history:

Received 31 May 2011

Accepted 28 June 2011

Available online 22 July 2011

Keywords:

EGCG

Nanogold

Bladder cancer

Anti-tumor activity

Immuno-stimulating activity

ABSTRACT

(–)-Epigallocatechin-3-gallate (EGCG), an active ingredient in green tea, was known to effectively inhibit formation and development of tumors. However, excessive uptake of EGCG was also known to cause cytotoxicity to normal cells. In this study, EGCGs that were physically attached onto the surface of nanogold particles (pNG) was confirmed by scanning electron microscopy. The anticancer activity of the EGCG-adsorbed pNG was investigated in C3H/HeN mice subcutaneously implanted with MBT-2 murine bladder tumor cells. EGCG–pNG was confirmed to inhibit tumor cell growing by means of cell apoptosis. The mechanism that EGCG–pNG mediates tumor apoptosis was uncovered to activate the caspase cascade through the Bcl-family proteins in the mitochondrial pathway. Additionally, the mechanism that tumors were suppressed by injecting EGCG–pNG directly into the tumor site was determined to be through downregulation of VEGF, whereas that by oral administration of EGCG was through reversing immune suppression upon cancer progression. In this assessment, the prepared EGCG–pNG was confirmed to be more effective than free EGCG in inhibiting bladder tumor in model mice.

© 2011 Elsevier Ltd. All rights reserved.

1. Introduction

Bladder cancer is one of the most common cancers. There were approximate 70,980 cases diagnosed with bladder cancer in the United States in 2009, of which 14,330 patients would likely succumb to the disease [1]. Intravesical chemotherapy by infusing drugs through urethra into bladder is the most common way to treat the early state bladder cancer. With the disease progressing, chemotherapy remains to be the main treatment before (neo-adjuvant therapy) or after (adjuvant therapy) cancer surgery. However, side effects, including abdominal pain, anemia, bladder irritation, blurred vision, excessive bleeding or bruising, fatigue, headache, infection, loss of appetite, nausea and vomiting, would arise, which can be severe [2].

Phytochemicals that arouse fewer side effects have emerged to be a new option as an effective chemotherapeutics for recalcitrant cancers [3,4]. (–)-Epigallocatechin-3-gallate (EGCG), an active ingredient in green tea, has been well documented to be actively

involved in prevention and treatment for many cancers, such as bladder, breast, prostate and colon cancers etc [4]. Epidemiological studies further pointed out that regular consumption of green tea is able to lower down risks of contracting given types of cancers, such as stomach, lung, colon, rectum, liver, breast and pancreas cancers [5,6]. Albeit EGCG has many desirable anti-tumorigenic properties as exemplified in human and animal models [7,8], some adverse effects, such as hepatitis, as a result of excessive consumption of EGCG have been reported [9]. Given these facts, taking EGCG as an anti-tumorigenic agent in clinics should ponder how to deliver EGCG to the right target site and to maintain an appropriate cell fluid level. It has been a thorny issue as to how to achieve the best EGCG pharmacodynamics and pharmacokinetics in cancer therapy.

Recently, nanoparticles that act as drug carriers drew great attention because nanoparticles possess unique physical properties, such as higher tissue permeability and colloidal stability, as well as relatively lower cost [10–13]. Drugs can be attached onto nanoparticles by means of ionic adsorption or covalent bonding. Nano gold particles (Nanogold, NG) otherwise were regarded as a safe drug delivery agent, which indeed have been constantly exploited [14,15]. For example, Chen et al. reported methotrexate-nanogold is

* Corresponding author. Tel.: +886 2 24622192x5137; fax: +886 2 24634203.

E-mail address: wuchangjer@yahoo.com.tw (C.-J. Wu).

¹ Dar-Shih Hsieh and Hang Wang contributed equally to this work.

more effective than free methotrexate in cancer treatment [16]. Additionally, VEGF-bound NG was reported to have anti-angiogenesis activity [17], which may result from reduction of chemical-induced macrophage infiltration and inflammation [18]. Moreover, NG has also been reported to be able to induce apoptosis in B-cell chronic lymphocytic leukemia (B-CLL) [19].

In this study, we aimed to develop clinically useful EGCG-conjugated nano gold particles in a hope to better treat bladder cancer. Meanwhile, we were also keen to know how EGCG–pNG acts.

2. Materials and methods

2.1. Cells culture and chemicals

MBT-2 murine bladder tumor cells were purchased from Japanese Collection of Research Bioresources (IFO50041, JCRB, Japan) and cultured according to Riggs et al. [20] with modifications. Briefly, cells were cultured in RPMI-1640 (GIBCO® Invitrogen, USA) supplemented with 10% fetal bovine serum (HyClone, Logan, Utah) and 50 U/ml penicillin/streptomycin (Gibco, Grand Island, New York). African green monkey kidney (Vero, ATCC CCL81) were maintained in RPMI-1640 medium supplemented with 5% fetal bovine serum. All cells were cultured at 37 °C in a humidified incubator with an atmosphere of 5% CO₂. EGCG (Taiyo Kagaku Co., Japan) and physical nanogold (pNG, Gold NanoTech, Inc., Taiwan) were added into individual or co-culture post ultrasound shaking by different concentrations for different periods.

2.2. Cell viability assay

For cell viability study, 1.5×10^4 cells resuspended in 100 µl medium were plated into each well of a 96-well plate for 24 h. The cells were then treated with different concentrations of the EGCG (0, 12.5, 25 and 50 µM) or pNG (0, 0.5, 1 and 2 ppm) or the combination for 24 or 48 h. Cell proliferation was monitored by using the CellTiter 96 Aqueous One Solution Assay and performed according to the manufacturer's instructions (Promega Corporation, USA). Briefly, after the treatment, 20 µl of the combined 3-(4,5-dimethylthiazol-2-yl)-5-(3-carboxymethoxyphenyl)-2-(4-sulfophenyl)-2H-tetrazolium inner salt (MTS) and phenazine methosulfate (PMS) solution was added into the wells containing 100 µl of culture medium, incubated for 40 min at 37 °C in a humidified, 5% CO₂ atmosphere. Record the absorbance at 490 nm using an ELISA plate reader. The concentration of EGCG and pNG that decreased cell count by 50% (IC50) was calculated by nonlinear least-squares curve fitting of experimental data.

2.3. Annexin V and cell cycle assay by flow cytometry

MBT-2 cells were incubated with or without EGCG (12.5, 25 and 50 µM) or pNG (0.5, 1 and 2 ppm) or combination for 24 h. The analysis of Annexin V binding was carried out with the Annexin V-FITC Detection Kit I (Roche Applied Science, Germany) according to the manufacturer's instructions. Briefly, cells were collected, washed twice with cold PBS, centrifuged at 1500 rpm for 5 min, and resuspended in $1 \times$ binding buffer. Then 10^5 cells were transferred to a 5-ml culture tube; 5 µl of Annexin V-FITC and 5 µl of PI were added. Cells were gently vortex-mixed, and incubated for 30 min at room temperature in the dark. Furthermore, 400 µl of $1 \times$ binding buffer were added to each tube, and samples were analyzed by FACScan flow cytometry (FACSort™, Becton Dickinson, USA). For each sample, 10,000 ungated events were acquired.

For cell cycle analysis, cells were collected, washed with cold PBS, fixed in cold (–20 °C) 100% ethanol, treated with DNase-free RNase, and stained with 50 µg/ml PI (Sigma, USA). Distribution of the cell-cycle phase with different DNA contents was determined with a flow cytometer. In each sample, 10,000 gated events were acquired. Analysis of cell-cycle distribution (including sub-G₀/G₁: apoptosis) was performed with CELLQuest software (Becton Dickinson Immunocytometry Systems, Mountain View, CA).

2.4. Western blot analysis

Confluent cell lines cultures were washed with buffered salt solution and treated with EGCG and/or pNG in the serum-free medium for 24 h. At the end of the experiments, medium was removed and 500 µl was concentrated using Microcon concentrators (Millipore, Bedford, MA) for 30 min at 25 °C. Concentrated samples with equal amounts of protein (25 µg) were mixed with 2 µl reducing sample buffer and resolved by SDS/PAGE, transferred to nitrocellulose membrane (Bio-Rad, Hercules, CA), and the blot was probed with polyclonal goat anti-mice Bcl-XL, Bad, Bax, VEGF and β-actin antibodies (Santa Cruz Biotechnology Inc.). Immunoreactive proteins were visualized by Immobilon™ Western chemiluminescent HRP Substrate kit (Millipore, MA, USA). Images were captured and the intensities of the protein bands were analyzed using the Labworks® software (V4.5, UVP Inc., Upland, CA, USA) are expressed as arbitrary optical density unit.

2.5. Mitochondrial membrane depolarization study by confocal microscopy

MBT-2 cells were grown in a 6-well tissue culture dish. The cells were either treated with 50 µM EGCG or combined 2 ppm pNG for 12 h. After treatment, the medium was replaced with serum-free medium containing 10 mg/ml JC-1, a potential-dependent J-1 aggregate forming lipophilic cation (Molecular Probes, Eugene, OR). Cells were incubated at 37 °C for 10 min followed by washing with PBS. Immediately, the cells were visualized by a confocal laser-scanning microscope (Leica SP2, Bannockburn, IL). The monomer and J-aggregate forms were simultaneously excited by 488-nm argon-ion laser sources [21]. Polarized mitochondria were marked by punctate orange-red fluorescence staining.

2.6. Caspase activity assay

MBT-2 cells were plated into 96-well plates with opaque sidewalls for this experiment. Cells were then treated were cultured with or without EGCG or pNG for 12 and 24 h. The Apo-ONE homogeneous caspase-3/7 assay substrate (Promega, Madison, WI) was utilized to evaluate the activities of caspase-3 and -7, effector caspases that cleave intracellular protein substrates triggering the apoptotic process. The caspase-3/7 substrate rhodamine 110, bis-(N-CBZ-L-aspartyl-L-glutamyl-L-valyl-L-aspartic acid amide; Z-DEVD-R110), is acted upon by caspase-3 and -7 resulting in a fluorescent leaving group. The amount of fluorescent product generated is proportional to the amount of caspase-3/7 cleavage activity present in the sample. Caspase-3/7 substrate was added to each well and incubated at room temperature for 1–2 h. A spectrofluorometer was used to measure fluorescence (excitation wavelength 485 ± 20 nm, emission wavelength 528 ± 20 nm).

2.7. Tumor model and experiment protocol

Male C3H/He mice at 6–8 weeks, were housed in a climate-controlled room (24 °C, 50 ± 10% relative humidity, 12-h light/12-h dark cycle, autoclaved bedding), with food (laboratory rodent diet, labdiet 5001, USA) and water *ad libitum*. Mice were divided into weight-matched groups: (1) tumor-bearing receiving water (Con), (2) tumor-bearing receiving 2 mg EGCG/mice (E) and (3) tumor-bearing receiving 2 mg EGCG plus 1.5 ppm pNG/mice (E + pNG). MBT-2 tumor cells (5×10^5) in a volume of 50 µl were injected subcutaneously into the right dorsal flank of C3H/He mice. Following inoculation of tumor cells or PBS, body mass, food intake and tumor size were measured four times weekly. Tumor growth was assessed by the measurement of two bisecting diameters in each tumor using calipers, and the tumor volume was calculated using the following equation, tumor volume (mm^3) = width \times length²/2.

Experiments are divided in two: First experiments designed to test the prevention and treatment effects of EGCG or combined with pNG. Mice from prevention category were given EGCG or combined with pNG by oral route once daily every other day for 7 days before MBT-2 cells implantation whereas treatment category started 14 days with a palpable nodule about mean volume of 197 ± 13 mm³ after tumor implantation. Second experiments designed to test the effects of different drug (EGCG combined with pNG, E + pNG) delivery strategies in cancer therapy. Administration of EGCG combined with pNG by oral (p.o.) or intraperitoneal (i.p.) or intratumor (i.t.) injection every other day on day 14 after tumor implantation.

2.8. Splenocyte isolation and NK cytotoxicity analysis

Splenocytes were isolated via centrifugation (300 g), and red blood cells were lysed using Gey's reagent (0.829 g NH₄Cl, 0.1 g HCO₃ and 3.72 mg Na₂EDTA in 100 ml ddH₂O). Splenocytes were washed twice with complete RPMI and viability was determined by trypan blue exclusion. To determine the NK cytotoxicity, cells were isolated from mouse spleen, and regard as effector cells. Stain the target cells (MBT-2) with DiOC18 (3,3'-dioctadecyloxacarbocyanine perchlorate) 10 µl per 1×10^6 cells. Incubation cells for 20 min at 37 °C, 5% CO₂. Wash the cells twice with buffer solution and resuspend in complete culture media at a concentration of 1×10^6 cells/ml. Prepare the target and effector cells (splenocytes) and made a co-culture of them with the desire ratio, i.e. E:T = 5:1; 20:1; 40:1. Incubate the co-culture for 4 h. Centrifuge the cell mixture at 250 g for 5 min after wash, discard supernatant. Washed and resuspend the cultured cells. Label the cells with propidium iodide (2 µl/per test) incubate at room temperature in dark. Analysis was performed using FACScan (FACSort™, Becton Dickinson, USA). For characterization of cell types, a large gate was drawn to include the monocyte and lymphocyte populations from forward scatter vs. side scatter.

2.9. Cytokine protein array

To assessment of cytokine of 4 groups, untreated and treated in MBT-2 bearing C3H mice, including control, tumor alone, tumor treated EGCG and EGCG + pNG. RayBio® Mouse Cytokine Antibody Array 1 (Cat. No. AAM-CYT-1, RayBiotech, USA) was used as protocol manuscript. Sera of each group, control, tumor-bearing, EGCG alone and EGCG mixed pNG, were collected and stored before sacrifice the mice. After blocking membranes with 2 ml $1 \times$ blocking buffer and incubate 1 to 2 h,

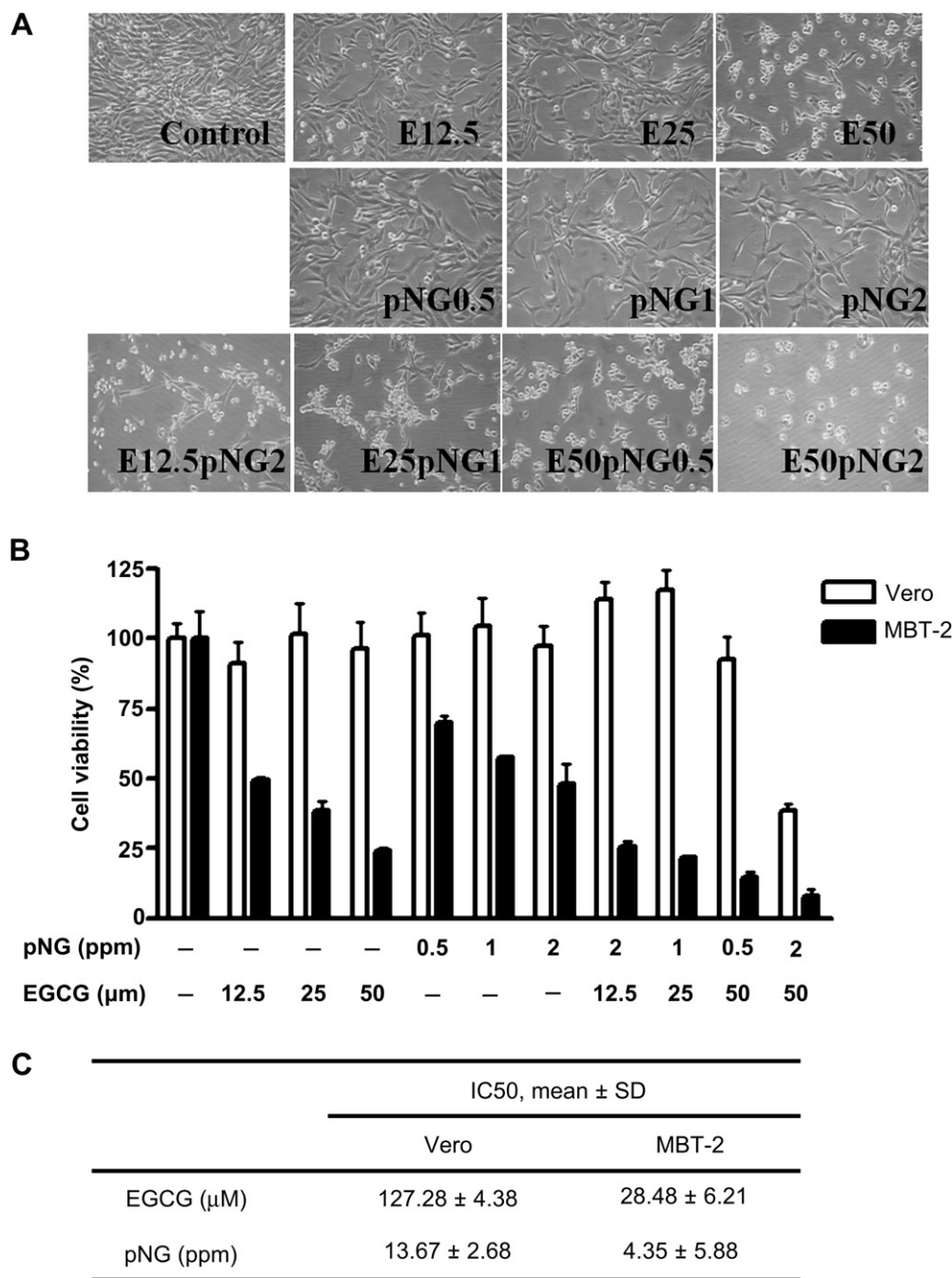


Fig. 1. pNG enhances cell growth inhibitory activity of EGCG. (A) MBT-2 cells were observed after treatment with or without 12.5–50 μM EGCG and/or 0.5–2 ppm NG for 48 h under an inverted microscope (magnification, $\times 200$). (B) MBT-2 and Vero cells (1.5×10^4 cells) were seeded into 96-well plates. After incubation for 24 h, the cells were incubated with the culture medium containing various concentrations of EGCG or pNG or combination for 48 h. The growth rates of MBT-2 and Vero cells were determined by the MTS assay. (C) EGCG and pNG mediated MBT-2 cells growth inhibition after 48 h. Experiments were performed in triplicate and values expressed as means \pm SD.

diluted 10-fold sera, 1 ml, was incubated with membranes of each group serum at room temperature for 4 $^{\circ}\text{C}$ for overnight. After 3 times buffer I and 2 times buffer II wash, biotin-conjugated anti-cytokines antibody (primary antibody) contained working solution was added in a tube container incubate at 4 $^{\circ}\text{C}$ for overnight. Then, 1000 fold dilute HRP-conjugated streptavidin was added for 4 $^{\circ}\text{C}$ overnight incubate post 3 times buffer I and 2 times buffer II wash. The detection and exposure were used ImmobilonTM Western chemiluminescent HRP Substrate (Millipore, MA, USA).

2.10. High-performance liquid chromatography

Qualitative of EGCG in EGCG–pNG complex was analyzed by HPLC. HPLC was performed according to the method published earlier with modifications [22]. The Waters HPLC system equipped with automated gradient controller, 510 pumps, U6K injector, 481 detector, 746 data module and Waters μ -bondapak C18 column

(3.9×300 mm), was used for the analysis. Elution was carried out at ambient temperature between 24 and 28 $^{\circ}\text{C}$ using water: methanol: acetic acid (70: 30: 0.5) as a mobile phase at a flow rate 1.0 ml/min. All extracts were prepared in triplicate and each extract was analyzed in triplicate. The UV detection was carried out at 280 nm.

2.11. Scanning electric microscopy (SEM)

EGCG and pNG were mixed post ultrasonic shaking, was store in freeze dryer (CRYODOS -50, TELSTAR, UK). Fixation and dehydration for the SEM are carried out. After dehydration by grading ethanols and drying, the samples are carefully mounted on an aluminum stub using either silver paint or a double stick carbon tape. Samples are then introduced into the chamber of the sputter coater and coated with a very thin film of gold/palladium before SEM examination. SEM was performed by Field Emission Scanning Transmission Electron Microscope-FE-STEM (Tecnai-G2-F20, FEI, USA).

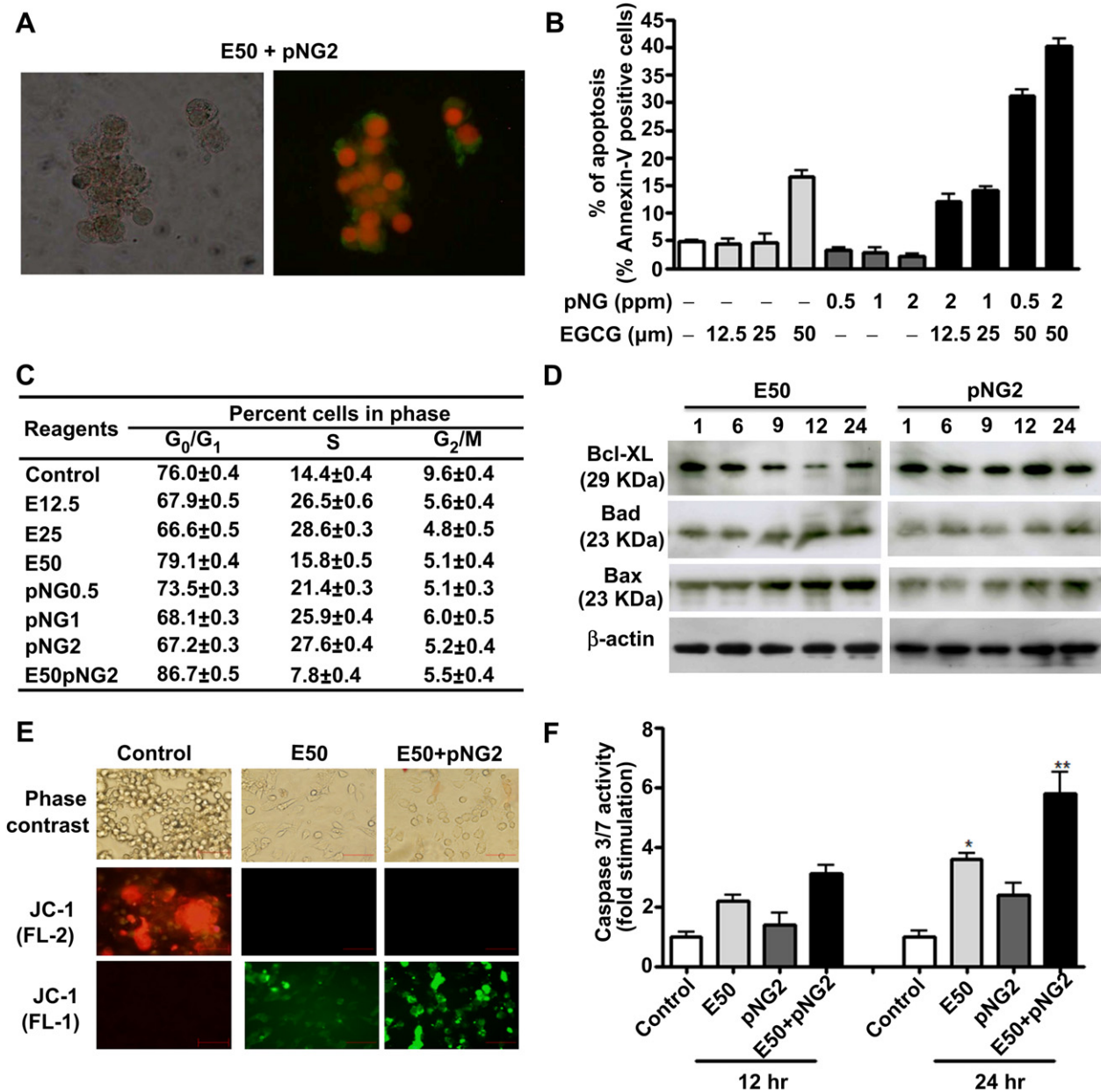


Fig. 2. pNG enhances anti-tumor effect of EGCG on bladder cancer cells through activating the caspase cascade. (A) Fluorescence microscopy of MBT-2 cells stained with Annexin V-FITC (Green) and PI (Red) after treatment with EGCG or combined with pNG for 48 h (magnification, $\times 400$). (B) Detection of apoptosis by Annexin V staining. MBT-2 cells were cultured with or without EGCG and/or NG for 24 h, followed by Annexin V staining. (C) The cell cycle of MBT-2 cells were analyzed by FACS. MBT-2 cells were treated with EGCG or NG for 24 h, followed by PI staining. (D) Bcl-2 family protein levels in MBT-2 cells exposed to the EGCG or NG for 24 h were analyzed by Western blot analysis. (E) Fluorescent images of JC-1 stained MBT-2 cells after 24 h EGCG or combined with pNG treatment (magnification, $\times 200$). (F) Caspase-3/7 activity after EGCG and/or NG treatment for 12 and 24 h. Data shown are means \pm S.D. for three samples. Data containing asterisk marks are significantly different from the values in control at $*p < 0.05$, $**p < 0.01$. (For interpretation of the references to color in this figure legend, the reader is referred to the web version of this article.)

2.12. Statistical analysis

Data were expressed as means \pm standard deviation. Statistical significance was determined by one-way ANOVA. Significance was accepted at the level of $p < 0.05$ (*), $p < 0.01$ (**), or $p < 0.001$ (***).

3. Results

3.1. In vitro anti-tumor activity of EGCG and pNG

To evaluate the tumor cytotoxicity of EGCG and/or pNG, we examined viabilities of bladder cancer cells (MBT-2) and African green monkey kidney cells (Vero cell acts as a normal cell) at 48 h

post-EGCG or -pNG treatment. EGCG and/or pNG were found to reduce the viability of MBT-2 cells in a concentration-dependent manner (Fig. 1A and B). The inhibitory concentrations at 50% effect level (IC₅₀) for EGCG and pNG against bladder cancer cell (MBT-2) lines were determined to be 28.4 μM and 4.3 ppm, respectively (Fig. 1C). In contrast, the Vero cell numbers were not changed in the presence of EGCG or pNG. To determine whether EGCG in conjunction with pNG has a synergistic effect on anti-tumorigenesis, we examined viable cell numbers after various combinations of EGCG and pNG were added into MBT-2 cell lines. The result turned out that EGCG and pNG in a combination of 12.5 μM and 2 ppm, respectively, significantly reduce MBT-2 cell numbers to 25.5% of control, whereas the cell numbers in the

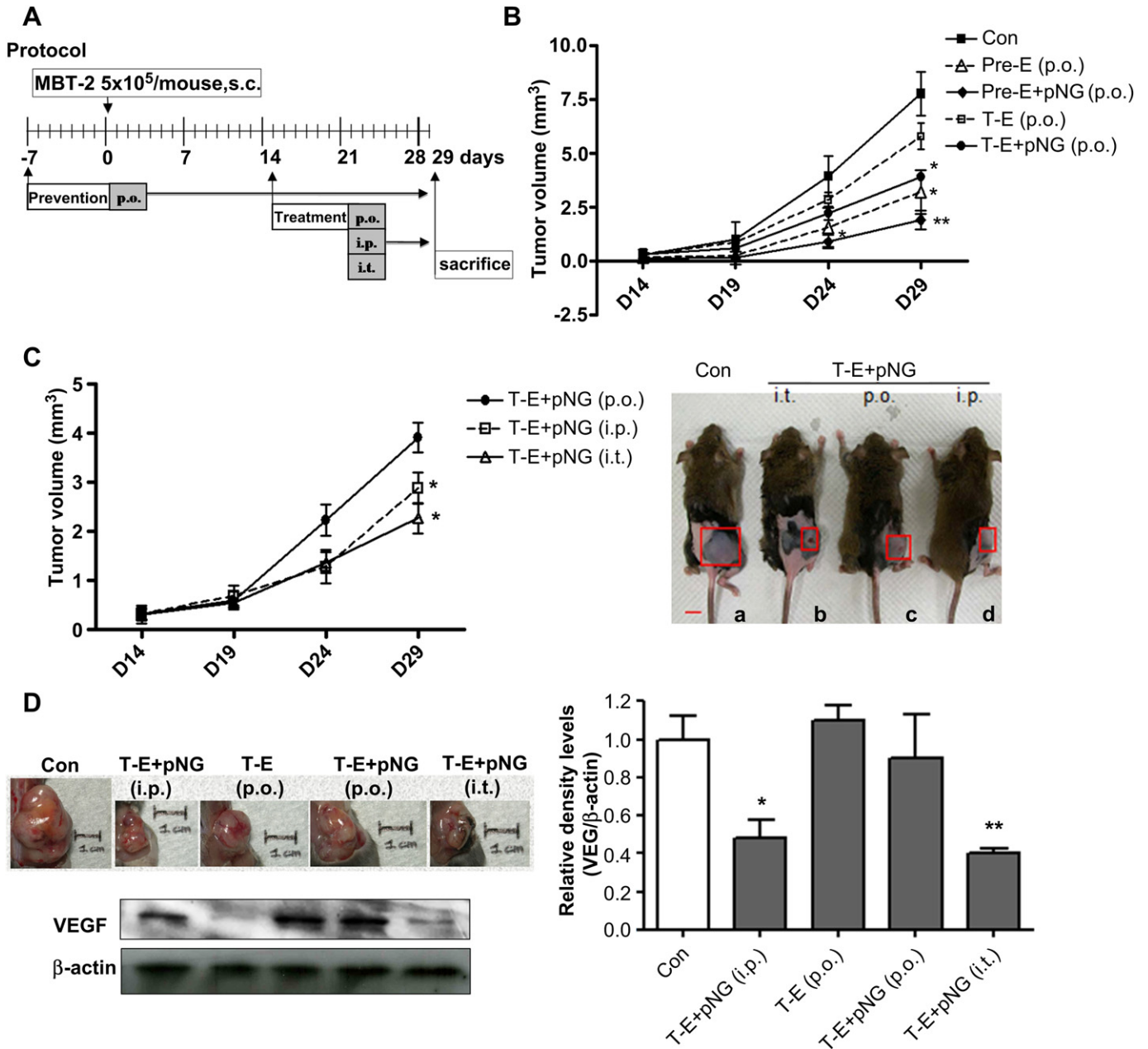


Fig. 3. Tumor growth and expression levels of VEGF after the treatment EGCG or combined with pNG *in vivo*. (A) Protocols for mouse bladder cancer model. Male mice were given EGCG or combined with pNG or water by oral route once daily every other day for 7 days before MBT-2 cells implantation in prevention experiment. In treatment experiment, mice were using oral (p.o.) or intraperitoneal (i.p.) or intratumor (i.t.) injection either water or EGCG or combined with pNG every other day on day 14 after tumor implantation. (B) The tumor volume in mice orally treated with EGCG and/or pNG. Tumor volumes were measured in two dimensions and calculated as follows: width \times length²/2. Each data point represents the mean \pm S.D. of tumor volumes from six animals and they are significantly different from control group at * $p < 0.05$, ** $p < 0.01$. (C) The tumor volume in mice from different drug (EGCG combined with pNG, E + NG) delivery strategies. Data containing asterisk marks are significantly different from the values in p.o. treatment group at * $p < 0.05$. (D) We excised tumors from mice 29 days after cell inoculation and photographed them (Upper left panel). Representative Western blot analyses of VEGF from each individual mouse. Levels of these proteins expression were normalized to β -actin (Lower left and right panel). Data containing asterisk marks are significantly different from the values in control at * $p < 0.05$, ** $p < 0.01$.

presence of EGCG or pNG alone were reduced to 49.7% and 48.1% of control, respectively (Fig. 1A and B). As a result, EGCG and pNG added together do have a synergistic effect on MBT-2 cell suppression.

3.2. The Effect of EGCG plus pNG treatment on induction of apoptosis in bladder cancer cells

Cell apoptosis features some morphological alterations, such as chromatin condensation, membrane blebbing, inter-nucleosomal

degradation of DNA, and apoptotic body formation. Previous study reported that EGCG can induce apoptosis via the PI3K/Akt pathway and Bcl-2 family proteins in T24 human bladder cancer cells [23]. To determine whether the tumor cell cytotoxicity of EGCG and/or pNG in MBT-2 cells is also mediated by the same mechanism, MBT-2 cells were first treated with EGCG (12.5, 25 and 50 μ M) or pNG (0.5, 1 and 2 ppm) for 24 h. The cells in test were subjected to flow cytometry analysis, whereby apoptotic bodies can be detected by Annexin V and PI staining. As a result, the cells treated with EGCG plus pNG were found to be apoptotic bodies

positive but those without treatment (Fig. 2A). The apoptotic cells resulted from EGCG and/or pNG treatments were quantified (%), for which MBT-2 cells were assayed using Annexin V. At 48 h, the percentage of Annexin V-positive cells was found to increase 2.5-fold, from 16.6% of cells with addition of EGCG to 40.2% of cells with addition of EGCG plus pNG (Fig. 2B).

As shown in Fig. 2A and B, pNG plus EGCG has a synergistic effect on MBT-2 apoptotic cell death. The mechanism of the EGCG and pNG mediated cell apoptosis was investigated. First, the MBT-2 cells that were treated with EGCG or pNG seemed to be arrested in the S phase of cell cycle (Fig. 2C). The MBT-2 cells otherwise underwent G₀/G₁ arrest when the doses of EGCG (50 μM) and pNG (2 ppm) were increased (Fig. 2C). Next, the protein expressions of Bcl-2 family in MBT-2 cells post-treated with EGCG or pNG were examined. As shown in Fig. 2D, Bcl-XL were expressed less at 9 h in the cells treated with EGCG; in the meantime the expressions of Bax started to increase. After 12 h, the levels of Bad and Bax in the cells treated with pNG were found to be slightly increased (Fig. 2C). These results indicated that Bcl-XL, Bad, and Bax are likely in connection with the EGCG and pNG mediated MBT-2 cell apoptosis.

Apoptosis has been related to the disruption of mitochondrial membrane integrity, which is critical in the cell-death process [24]. JC-1, a cationic dye, can potential-dependently reside inside mitochondria of healthy cells. Excessive cationic dyes would form red aggregates that feature a characteristic fluorescence emission shift from green to red. When mitochondria depolarized, JC-1 would leak out of mitochondria to surroundings, whereby the dye aggregates become less. In the MBT-2 cells receiving no treatment, mitochondria was heterogeneously distributed and the spectrum was profiled with typical low intensity of green fluorescence (JC-1 monomers) and high intensity of red fluorescence (JC-1 aggregates). However, the spectrum profile reversed in the cells treated with EGCG or EGCG plus pNG (Fig. 2E).

To be sure that the EGCG and pNG mediated apoptosis is triggered by the caspase effectors, we then examined expressions of the apoptosis-dependent enzymes caspase-3 and -7. The expressions of caspase-3 and -7 were found to significantly increase, when MBT-2 cells were treated with EGCG (Fig. 2F). And, the expressions of caspase-3 and -7 in the cells treated with the combination of EGCG and pNG (5.81 ± 0.70-fold increase versus the vehicle-alone controls, $p < 0.01$) were found to be relatively higher than that treated with EGCG alone (2.42 ± 0.43-fold increase, $p < 0.05$) (Fig. 2F).

3.3. In vivo anti-tumor activity of EGCG and pNG

Since EGCG–pNG has been shown to be effective in suppressing the growth of tumor cells *in vitro*, we went on to examine its efficacy and safety *in vivo*. Mice were first implanted with MBT-2 cells and then treated with EGCG or EGCG–pNG (Fig. 3A). In the early and late intervention, EGCG and/or pNG were administered orally in mice (Fig. 3B). The result showed that only can the combined treatment significantly reduce the tumor volume after 24 days for the mice implanted with the cancer graft. Additionally, the mean tumor volume was significantly reduced in the prevention and treatment groups that received the combined treatment (75% and 50%, respectively, at day 29).

To assess the delivery efficacy on the cancer therapy, the mice implanted with MBT-2 cells were subjected to administration of EGCG plus pNG orally (p.o.), intraperitoneally (i.p.) or intratumor (i.t.) every other day after two weeks of tumor cells inoculation. There was no difference in food uptake and body weight among the testing groups (data not shown). Other physiological parameters (i.e., liver, kidney, spleen, and uterine weight) were also no detectable difference. The growth-suppressive effect of EGCG plus pNG was found to be more effective in the group via i.t. or i.p. than

that via p.o. (Fig. 3C). Whether the better tumor suppression by means of i.t. or i.p. is result of downregulation of VEGF was determined. Expressions of VEGF in tumor cells were assayed by Western blotting; as shown in Fig. 3D the levels of VEGF in the tumor cells were found to be influenced by either i.t. or i.p. administration of the combination (EGCG plus pNG) but not by p.o. As a result, the anti-tumor effect via injection of EGCG plus pNG is correlated to the suppression of VEGF.

3.4. Immunomodulating effects after EGCG plus pNG treatment

Whether the reduction of tumor size is dependent on active immune response was examined by determining cytokine levels and NK associated cytotoxicity. Relative protein levels of 8 cytokines were determined by using a cytokine antibody array system. The relative expression levels in experimental groups were compared with those of control as shown in Fig. 4A. The expression levels of interleukin-4 (IL-4) and IL-6 significantly decreased ($p < 0.01$ and $p < 0.05$, respectively) in the group administrated orally with the combination of EGCG and pNG, while the expression levels of IL-2 and interferon-γ (IFN-γ) increased markedly. So, the anti-tumor effect of EGCG plus pNG via oral administration can be correlated to the cell-mediated immunity and natural killer (NK)-cell activity. To verify this hypothesis, we examined cytotoxic activity of NK cells in the tumor-bearing mice by staining MBT-2 cells with two fluorescent dyes, DIOC18 and propidium iodide (PI). On this basis, the E/T ratio was determined to be 50/1 in the

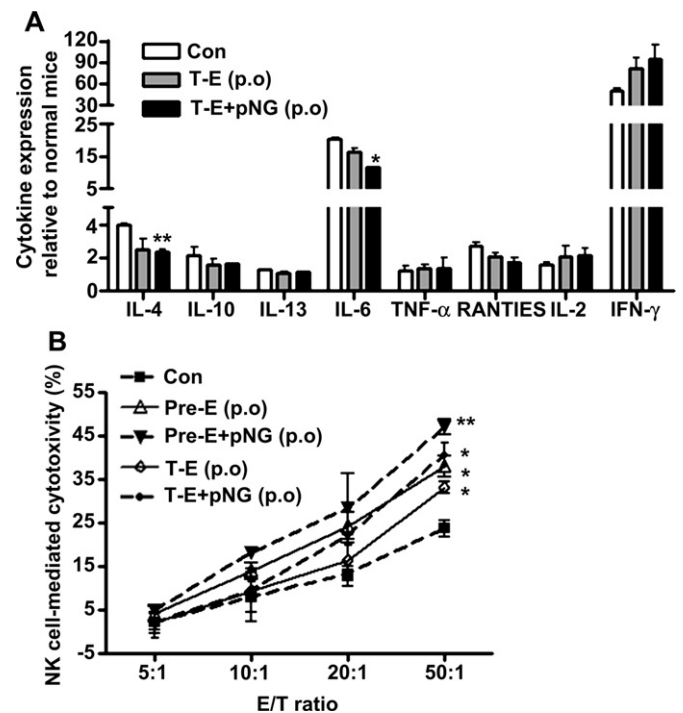


Fig. 4. pNG enhances EGCG altered immunological functions in tumor-bearing mice. (A) Serum cytokine levels were determined by mice protein array ($n = 5-8$ mice per group from two independent experiments). Levels of these cytokines expression were normalized with the expression in normal mice (non-tumor) being regarded as 1. Each bar represents the mean and standard deviation of values obtained from different mice. Each data point represents the mean ± S.D. of serum levels from six animals and they are significantly different from control group at * $p < 0.05$, ** $p < 0.01$. (B) Tumor-bearing mouse were fed with EGCG and pNG for the experimental period. After sacrifice, NK cytotoxicity was assayed in spleen cells from prevention and treatment experiments. The splenocytes from C3H/He mice were used as the effector cells to test the protective effect of experimental diets for the NK associated cytotoxicity against target cells (line-1).

group subject to early intervention of EGCG plus pNG (Pre-E + pNG), which corresponded to the maximal effect of NK cytotoxicity (45% MBT-2 cells were stained with PI, $p < 0.01$, Fig. 4B).

3.5. Characterization of EGCG–pNG complex

Next, we measured some physical properties for the EGCG–pNG complex and formulated the best combination. EGCG released from the complex by ultrasound vibration (UV) was found to be less than that by vertex vibration (V) (Fig. 5A), suggesting that the preparation of EGCG–pNG complex by UV is more appropriate. The zeta potential of EGCG–pNG was also found to increase to $+21.0 \pm 5.0$ mV, indicating that EGCG is attached onto the surface of pNG (Fig. 5B). To be sure, we analyzed freeze-dried crystals of the complex by SEM, whereby the EGCG–pNG complex was found to have low conductivity. In light of white precipitates (pNG) overlying clusters of black grains (EGCG–pNG complex), the low conductivity is likely as a result of EGCG coating (an insulator) (Fig. 5C). On this basis, we proposed a model for the formation of the complex as detailed in Fig. 5D.

4. Discussion

4.1. Physical nanogold (pNG) induced cell growth inhibitory activity of EGCG through enhancing apoptosis

Recent studies have shown a positive cause-effect relationship between green tea-containing supplements and liver damage

[9,25]. That consumption of green tea-derived supplements at a high dose has toxic effects has been manifested in rodents [26]. However, in this study we found that an appropriate formulation of EGCG and metal nanoparticle can avoid such an unwanted outcome but still preserve the wanted anti-tumor activity. The fact is we have established that physical nanogold (pNG) in conjunction with EGCG is safe and effectively inhibit tumor growth through regulations of angiogenesis and host immunity.

The biological activity of EGCG that can be enhanced by associating with heavy metals such as Zn^{2+} , Cd^{2+} and Cu^{2+} was previously noted in a number of reports [27–29]. For example, EGCG-associated heavy metals to induce tumor cell necrosis or apoptosis were hypothesized [30]. In spite of the true mechanism was unknown; we demonstrated herein that the combination of EGCG and pNG that can suppresses bladder tumor growth in mice is through mitochondria-mediated apoptotic pathway (Fig. 1) and has no observable side effects. We also demonstrated that the EGCG–pNG mediated apoptosis in the MBT-2 cells is triggered by activating the caspase cascade of the mitochondrial pathway, whereby the cell arresting takes place in the G_0/G_1 phase of the cell cycle (Fig. 2).

Yang et al. [27] reported that the biological activity of EGCG was altered in the presence of metals. We reasoned that the alteration may be as a result of forming EGCG–metal complexes which likely change free radical levels in cells. So, free radical should play an important role in the EGCG–pNG mediated apoptosis. Additionally, the entry of pNG into cells was hypothesized to proceed via the path of receptor-mediated endocytosis [31].

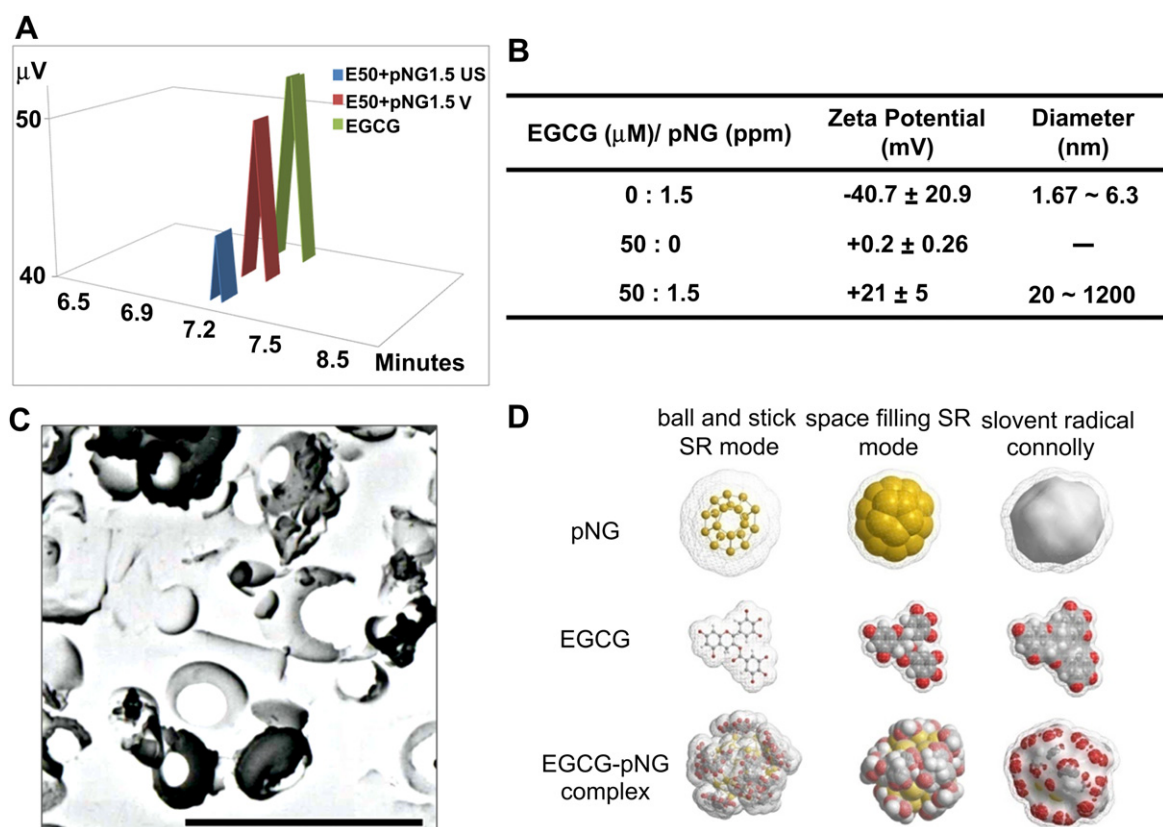


Fig. 5. Characterization of EGCG–pNG complex (A) Un-conjugated EGCG was detected by HPLC. EGCG–pNG complexes were prepared as follows: 50 μM EGCG and 1.5 ppm pNG were added to sodium phosphate buffer. The solution was then mixed by ultrasound (UV) or vertex vibration (V), followed by centrifugation to separate unadsorbed EGCG from EGCG–pNG conjugates. (B) Particle size and zeta potential of EGCG and/or pNG complex. After prepared EGCG–pNG complexes by ultrasound vibration (UV), zeta potential and particle size of pNG were increased to $+21.0 \pm 5.0$ mV and 20–1200 nm, respectively. (C) EGCG–pNG complexes were detected in SEM. Combination of 50 μM EGCG and 1.5 ppm pNG post frozen-dry crystallization was detected about 1 μm in SEM (20 KV, 5000×). EGCG (black) can be conjugated on the surface of pNG (white). Bar scale: 3 μm. (D) Prediction of assembling the complex by Software (Chem3D ultra 8.0). From the speculated the structure of EGCG–pNG complex, drug–nanoparticle was conjugate by grafting EGCG to the surface of pNG.

4.2. Combined EGCG and pNG treatment attenuates VEGF expression and prevents the loss of natural killer cell activity in tumor-bearing mice

When EGCG and/or pNG were given orally, the suppression of tumor growth is more pronounced in a prevent condition (Fig. 3B). Recently, pNG was shown to have the anti-angiogenesis activity [17]. Although the VEGF levels in the mice orally administered with EGCG–pNG made no difference from those in the mice treated with the vehicle control, the VEGF level in the mice directly injected with the EGCG–pNG complex does decrease significantly (Fig. 3D). So, the anti-tumor effect of the EGCG–pNG complex may be linked to VEGF suppression to some extent.

It is now clear that the formation of pre-malignant and malignant tissues is associated with the impairments of immune cells. According to the immunosurveillance hypothesis, NK cells are known to directly engage in tumor killing (via perforin, granzyme B, TRAIL, or FasL-dependent mechanisms), but Th1 (by virtue of IFN- γ production) and Th17 cells (via production of IL-17A) also provide considerable assistances to boost cytotoxic immunity [32–34]. Pre-malignant and malignant tissues are known in association with the suppression of the Th1 responses as well as the activation of the Th2 responses. In the peripheral blood of bladder and colorectal cancer patients, the proportions of Th1 cells (to produce IFN- γ or IL-2) are significantly decreased, whereas the proportions of Th2 cells (that produce IL-4, IL-6 and/or IL-10) are significantly increased [35,36]. Since the levels of IL-4 and tumor growth were low (Figs. 4A and 3B), EGCG and/or pNG was considered to effect by modulating the immune system of hosts. In fact, the NK associated cytotoxicity was identified here (Fig. 4B).

5. Conclusions

pNG was determined to be able to activate caspase signaling by altering the ratio of Bax/Bcl-2 as well as mitochondrial membrane integrity. Inhibition of tumor cells by EGCG–pNG complex is achieved via the mechanism of cell apoptosis. Additionally, the EGCG–pNG complex can lower the level of VEGF so as to boost anti-tumor immunity. EGCG in conjunction with pNG does exert a synergistic effect to outperform individuals in anti-tumorigenesis.

Acknowledgments

The authors thank the Gold NanoTech, Inc., Taiwan for kindly providing physical nanogold particles. We also like to thank Dr. Tsung-Lin Li of Academia Sinica for many valuable suggestions.

References

- [1] Jemal A, Siegel R, Ward E, Hao Y, Xu J, Thun MJ, et al. Cancer statistics, 2009. *CA Cancer J Clin* 2009;59(4):225–49.
- [2] Taylor JH, Davis J, Schellhammer P. Long-term follow-up of intravesical bacillus calmette-guerin treatment for superficial transitional-cell carcinoma of the bladder involving the prostatic urethra. *Clin Genitourin Cancer* 2007;5(6):386–9.
- [3] Shankar S, Ganapathy S, Srivastava RK. Green tea polyphenols: biology and therapeutic implications in cancer. *Front Biosci* 2007;12:4881–99.
- [4] Yang CS, Wang X, Lu G, Picinich SC. Cancer prevention by tea: animal studies, molecular mechanisms and human relevance. *Nat Rev Cancer* 2009;9(6):429–39.
- [5] Lin JK, Liang YC. Cancer chemoprevention by tea polyphenols. *Proc Natl Sci Counc Repub China B* 2000;24(1):1–13.
- [6] Hsu SD, Singh BB, Lewis JB, Borke JL, Dickinson DP, Drake L, et al. Chemoprevention of oral cancer by green tea. *Gen Dent* 2002;50(2):140–6.
- [7] Beltz LA, Bayer DK, Moss AL, Simet IM. Mechanisms of cancer prevention by green and black tea polyphenols. *Anticancer Agents Med Chem* 2006;6(5):389–406.
- [8] Mukhtar H, Ahmad N. Tea polyphenols: prevention of cancer and optimizing health. *Am J Clin Nutr* 2000;71(6 Suppl):1698S–702S. discussion 1703S–1694S.
- [9] Mazzanti G, Menniti-Ippolito F, Moro PA, Casseti F, Raschetti R, Santuccio C, et al. Hepatotoxicity from green tea: a review of the literature and two unpublished cases. *Eur J Clin Pharmacol* 2009;65(4):331–41.
- [10] Nie S, Emory SR. Probing single molecules and single nanoparticles by surface-enhanced raman scattering. *Science* 1997;275(5303):1102–6.
- [11] Rosi NL, Giljohann DA, Thaxton CS, Lytton-Jean AK, Han MS, Mirkin CA, et al. Oligonucleotide-modified gold nanoparticles for intracellular gene regulation. *Science* 2006;312(5776):1027–30.
- [12] Sperling RA, Rivera Gil P, Zhang F, Zanella M, Parak WJ. Biological applications of gold nanoparticles. *Chem Soc Rev* 2008;37(9):1896–908.
- [13] Grzelczak M, Perez-Juste J, Mulvaney P, Liz-Marzan LM. Shape control in gold nanoparticle synthesis. *Chem Soc Rev* 2008;37(9):1783–91.
- [14] Stone J, Jackson S, Wright D. Biological applications of gold nanorods. *Wiley Interdiscip Rev Nanomed Nanobiotechnol* 2011;3(1):100–9.
- [15] Patra HK, Banerjee S, Chaudhuri U, Lahiri P, Dasgupta AK. Cell selective response to gold nanoparticles. *Nanomedicine* 2007;3(2):111–9.
- [16] Chen YH, Tsai CY, Huang PY, Chang MY, Cheng PC, Chou CH, et al. Methotrexate conjugated to gold nanoparticles inhibits tumor growth in a syngeneic lung tumor model. *Mol Pharm* 2007;4(5):713–22.
- [17] Mukherjee P, Bhattacharya R, Wang P, Wang L, Basu S, Nagy JA, et al. Anti-angiogenic properties of gold nanoparticles. *Clin Cancer Res* 2005;11(9):3530–4.
- [18] Tsai CY, Shiau AL, Chen SY, Chen YH, Cheng PC, Chang MY, et al. Amelioration of collagen-induced arthritis in rats by nanogold. *Arthritis Rheum* 2007;56(2):544–54.
- [19] Mukherjee P, Bhattacharya R, Bone N, Lee YK, Patra CR, Wang S, et al. Potential therapeutic application of gold nanoparticles in B-chronic lymphocytic leukemia (BCLL): enhancing apoptosis. *J Nanobiotechnology* 2007;5:4.
- [20] Riggs DR, DeHaven JI, Lamm DL. Allium sativum (garlic) treatment for murine transitional cell carcinoma. *Cancer* 1997;79(10):1987–94.
- [21] Smiley ST, Reers M, Mottola-Hartshorn C, Lin M, Chen A, Smith TW, et al. Intracellular heterogeneity in mitochondrial membrane potentials revealed by a J-aggregate-forming lipophilic cation JC-1. *Proc Natl Acad Sci U S A* 1991;88(9):3671–5.
- [22] Lee MJ, Prabhu S, Meng X, Li C, Yang CS. An improved method for the determination of green and black tea polyphenols in biomatrices by high-performance liquid chromatography with coulometric array detection. *Anal Biochem* 2000;279(2):164–9.
- [23] Qin J, Xie LP, Zheng XY, Wang YB, Bai Y, Shen HF, et al. A component of green tea, (–)-epigallocatechin-3-gallate, promotes apoptosis in T24 human bladder cancer cells via modulation of the PI3K/Akt pathway and Bcl-2 family proteins. *Biochem Biophys Res Commun* 2007;354(4):852–7.
- [24] Green DR, Reed JC. Mitochondria and apoptosis. *Science* 1998;281(5381):1309–12.
- [25] Bonkovsky HL. Hepatotoxicity associated with supplements containing Chinese green tea (*Camellia sinensis*). *Ann Intern Med* 2006;144(1):68–71.
- [26] Galati G, Lin A, Sultan AM, O'Brien PJ. Cellular and in vivo hepatotoxicity caused by green tea phenolic acids and catechins. *Free Radic Biol Med* 2006;40(4):570–80.
- [27] Yang JG, Yu HN, Sun SL, Zhang LC, He GQ, Das UN, et al. Epigallocatechin-3-gallate affects the growth of LNCaP cells via membrane fluidity and distribution of cellular zinc. *J Zhejiang Univ Sci B* 2009;10(6):411–21.
- [28] Yu HN, Yin JJ, Shen SR. Growth inhibition of prostate cancer cells by epigallocatechin gallate in the presence of Cu²⁺. *J Agric Food Chem* 2004;52(3):462–6.
- [29] Yu HN, Shen SR, Yin JJ. Effects of interactions of EGCG and Cd(2+) on the growth of PC-3 cells and their mechanisms. *Food Chem Toxicol* 2007;45(2):244–9.
- [30] Yang J, Yu H, Sun S, Zhang L, Das UN, Ruan H, et al. Mechanism of free Zn(2+) enhancing inhibitory effects of EGCG on the growth of PC-3 cells: interactions with mitochondria. *Biol Trace Elem Res* 2009;131(3):298–310.
- [31] Alkilany AM, Nagaria PK, Hexel CR, Shaw TJ, Murphy CJ, Wyatt MD, et al. Cellular uptake and cytotoxicity of gold nanorods: molecular origin of cytotoxicity and surface effects. *Small* 2009;5(6):701–8.
- [32] Dunn GP, Old LJ, Schreiber RD. The immunobiology of cancer immunosurveillance and immunoeediting. *Immunity* 2004;21(2):137–48.
- [33] Dunn GP, Koebel CM, Schreiber RD. Interferons, immunity and cancer immunoeediting. *Nat Rev Immunol* 2006;6(11):836–48.
- [34] Martin-Orozco N, Muranski P, Chung Y, Yang XO, Yamazaki T, Lu S, et al. T helper 17 cells promote cytotoxic T cell activation in tumor immunity. *Immunity* 2009;31(5):787–98.
- [35] Agarwal A, Verma S, Burra U, Murthy NS, Mohanty NK, Saxena S, et al. Flow cytometric analysis of Th1 and Th2 cytokines in PBMCs as a parameter of immunological dysfunction in patients of superficial transitional cell carcinoma of bladder. *Cancer Immunol Immunother* 2006;55(6):734–43.
- [36] Kanazawa M, Yoshihara K, Abe H, Iwadata M, Watanabe K, Suzuki S, et al. Effects of PSK on T and dendritic cells differentiation in gastric or colorectal cancer patients. *Anticancer Res* 2005;25(1B):443–9.